Protons from ^{8}B+^{58}Ni

E.F. Aguilera[a,b,*], E. Martinez-Quiroz[a], H. García-Martínez[a,b], D. Lizcano[a], J. J. Kolata[c], L. O. Lamm[c],
G. Rogachev[c], P.A. DeYoung[d], C. Guess[d], U. Khadka[d], P.J. Mears[d], F.D. Becchetti[e],
Y. Chen[e], H. Jiang[e], J.D. Hinnefeld[f], and G.F. Peaslee[g]
[a]Departamento del Acelerador, Instituto Nacional de Investigaciones Nucleares,
Apartado postal 18-1027, 11801, México, D.F., México.
[b]Universidad Autónoma del Estado de México, C.P. 50000, Toluca, México.
[c]Physics Department, University of Notre Dame,
Notre Dame, In, 46556-5670
[d]Department of Physics and Eng., Hope College,
Holland, Mi, 49423-9000
[e]Physics Department, University of Michigan,
Ann Arbor, Mi, 48109-1120
[f]Physics Department, Indiana University South Bend,
South Bend, In, 46694-7111
[g]Department of Chemistry, Hope College,
Holland, Mi, 49423-9000

Proton angular distributions are measured for the exotic proton-halo nucleus ^{8}B on a ^{58}Ni target. The proton spectra are well described by statistical model calculations using the code PACE if both complete and incomplete fusion are taken into account. Fusion cross sections are deduced by using calculated proton multiplicities, a technique that is first successfully tested with the better known beam ^{6}Li. The resulting fusion excitation function shows a large enhancement that requires a strikingly large barrier radius in order to be described, consistent with the assumption of a proton halo for ^{8}B.

Keywords: Exotic nucleus; proton halo; complete and incomplete fusion.

Se midieron las distribuciones de protones producidos en la reacción del núcleo con halo protónico ^{8}B con ^{58}Ni. Si toma en cuenta tanto fusión completa como incompleta, los espectros de protones son bien descritos con el modelo estadístico implementado en el código PACE. Las secciones eficaces de fusión se deducen, usando las multiplicidades predichas. Primero se verificó la validez del método usando, aplicándolo en forma satisfactoria para un proyectil de ^{6}Li. La función de excitación obtenida, presenta un acercamiento grande, que para ser descrito, requiere de un valor sorprendentemente grande del radio de la barrera, lo cual es consistente con la suposición del halo protónico para el ^{8}B.

Descriptores: Núcleo exótico; halo protónico; fusión completa e incompleta.

PACS: 25.60.-t; 25.60.Pj; 25.70.-z

1. Introduction

The radioactive nucleus ^{8}B is adjacent to the proton drip line and has a very small proton separation energy (0.138 MeV). In addition to its role in the production of high-energy neutrinos in the sun [1, 2], it attracted much attention in the last decade because of the proposal that it might have a proton halo [3, 4]. Recent work at the University of Notre Dame [5, 6] has established the exotic, proton-halo nature of this nuclide. In Ref. [5], the angular distribution for the breakup of ^{8}B on a ^{58}Ni target was measured and it was found that Coulomb-nuclear interference at very large distances still plays an important role, which was taken as evidence for the proton-halo nature. Even for distances of closest approach larger than 30 fm, the nuclear effect was found to be important.

In contrast to nuclei with a proton-halo, neutron-halo nuclei have been more widely investigated, as is the case for ^{6}He, which has been extensively studied in recent years [7–11]. It would be interesting to compare the sub-barrier fusion and transfer/breakup yields for ^{8}B+^{58}Ni with the observations of these reaction mechanisms for ^{6}He+^{209}Bi [7–11], where large enhancements are observed below the barrier, in this case presumably due to the neutron-halo structure of ^{6}He.

As for other proton-halo nuclei, Rehm et al. [12] have studied the fusion of ^{17}F+^{208}Pb and found a slightly reduced fusion cross section below the barrier. Liang, et al. [13] have measured breakup of ^{17}F on ^{208}Pb and found a very small cross section. It is not clear, however, that either of these experiments gives relevant information on the effect of the proton-halo state, which is an excited state in ^{17}F. The probability of Coulex to the halo state during the fusion reaction is very small [12], so the proton halo likely did not come into play.

Also, the breakup experiment was performed at an energy well above the Coulomb barrier, and in an angular range where absorption via the imaginary part of the optical potential is very large, so peripheral breakup, which is sensitive to the halo state, was not being probed.

So, it is far from clear that enhanced cross sections should be expected in the proton halo case.

The reduced Coulex probability in ^{8}B breakup is at least partly due (in semi-classical terms) to "polarization" of the projectile via the Coulomb force, resulting in the valence proton spending more time at large distances from the target, where it is shielded by the core from the full Coulex effect.

This would also tend to keep transfer and fusion yields near those of the core. In contrast, Coulomb polarization favors neutrons in the halo residing in the region between the core and the target, which then enhances the reaction probabilities as we have observed. Of course, semi-classical arguments like these are suspect for quantum systems, but this serves to emphasize that fusion, transfer, and breakup yields near the barrier need to be studied for true proton-halo systems.

Thus, we proposed to measure the fusion-evaporation cross sections for ^{8}B+^{58}Ni, in a kinematic regime that emphasizes peripheral reactions. These data could then be compared with our ^{6}He+^{209}Bi yields, and to the breakup data observed previously for ^{8}B+^{58}Ni [5], where nuclear processes presumably play a much bigger role. Finally, it will be important to compare the measured fusion and breakup yields with those for the core nucleus, ^{7}Be.

This work presents preliminary results as part of an experimental program including a series of measurements aimed to clarify the role of the proton-halo wave function of ^{8}B as it relates to reaction cross sections at near barrier energies.

2. Experimental procedure

The ^{8}B beam was obtained from primary ^{6}Li projectiles through the reaction ^{3}He(^{6}Li,n)^{8}B using the radioactive beam facility TwinSol at the University of Notre Dame [14]. A test experiment was first performed with a natural Ni target (1.36 mg/cm^2) using 36 and 38 MeV for the primary ^{6}Li-beam. In a second stage, ^{8}B projectiles generated with 32, 34 and 36 MeV primary beams were used to bombard an enriched ^{58}Ni target with a thickness of 0.924 mg/cm^2. A bunched beam was used in order to identify the reaction products by time-of-flight.

The experimental arrangement is shown schematically in Fig. 1. Four ΔE-E Silicon surface-barrier telescopes were used at backward angles to detect the evaporated protons from the fused system, while two telescopes at forward angles served to monitor the beam.

Before starting the experiment, another telescope with a position sensitive detector (PSD) was used in the target position to characterize the beam. The beam intensity was reduced by a factor of 10^3 during the characterization and the telescope was taken away during the real experiment. A sample of the beam spectrum is shown in Fig. 2, where the main beam components (^{6}Li,^{7}Be,^{8}B) are clearly separated by
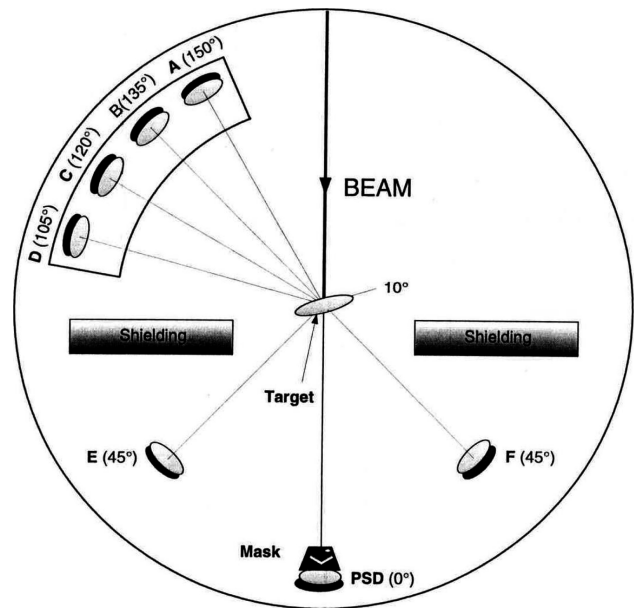

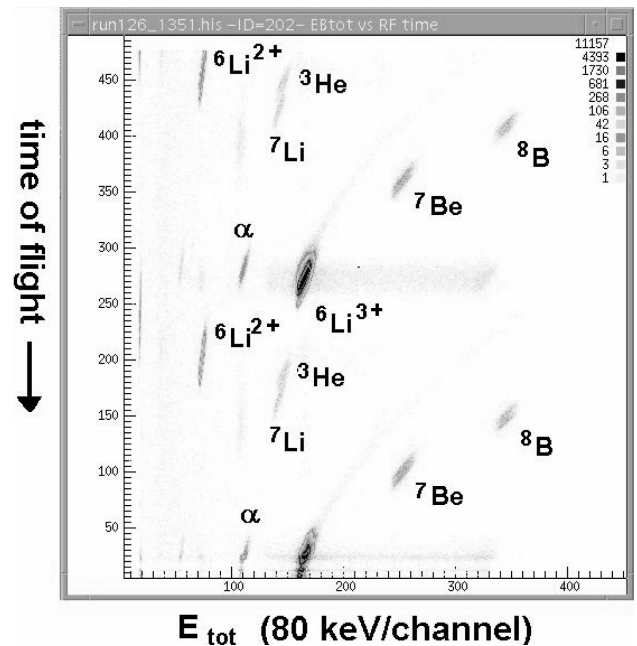FIGURE 1. Experimental arrangement.

FIGURE 2. Beam composition.

time-of-flight. So, even though the ^{6}Li component is much stronger (approximate ratios are 150:1.5:1, respectively) the possible mixture of corresponding reaction products is not a concern. A small contamination due to the ^{7}Li component of the beam might be present in the proton yield associated to ^{8}B since the corresponding times-of-flight are similar. In contrast to ^{8}B, however, the ^{7}Li beam energies are always below the corresponding Coulomb barrier. This, combined with the fact that proton multiplicities for ^{7}Li+^{58}Ni are about a factor of 2 lower than the ones for the ^{8}B beam, leads to a negligible effect (about 1%) on the proton yields.

Proton multiplicities calculated with the code PACE [15] were used to estimate the fusion cross sections. In order to test the technique, the fusion with the contaminant beam ^{6}Li (Fig. 2) was first analyzed. Being ^{6}Li a stable nucleus, this is a much better known beam and there is the additional advantage that we can compare to the measurements reported for the neighboring system ^{6}Li+^{59}Co Ref. [16].

3. Results and Discussion

The three proton angular distributions, obtained for ^{6}Li+^{58}Ni (enriched target) at $E_{c.m.}$=11.0, 11.6 and 12.2 MeV, are presented in Fig. 3, while Fig. 4 shows a sample spectrum, taken with the θ_{lab}=135.8^0 detector at $E_{c.m.}$=12.2 MeV.

The PACE calculations displayed in the latter figure were made considering that ^{6}Li can be viewed as formed by two clusters (^{4}He+^{2}H). They describe the data quite well indi-

cating that, in addition to complete fusion (CF), some incomplete fusion (ICF) might be contributing to the proton production. This in spite that any interference between the different contributions has been neglected. Proton angular distributions in the laboratory system, as predicted by PACE, show a slight tendency to increase at small angles but are quite flat in the angular region of our measurements, in agreement with Fig. 3.

The reasonably good PACE description of experimental data for both the spectra and the angular distributions, strongly support the hypothesis that the observed protons were actually produced in the fusion-evaporation process, so that fusion cross sections can be extracted from the data by using the proton multiplicities calculated with PACE (see Table I).

The corresponding excitation function is presented in Fig. 5, where the curve represents the data for ^{6}Li+^{59}Co [16], properly scaled by the radius and barrier for the ^{58}Ni target.

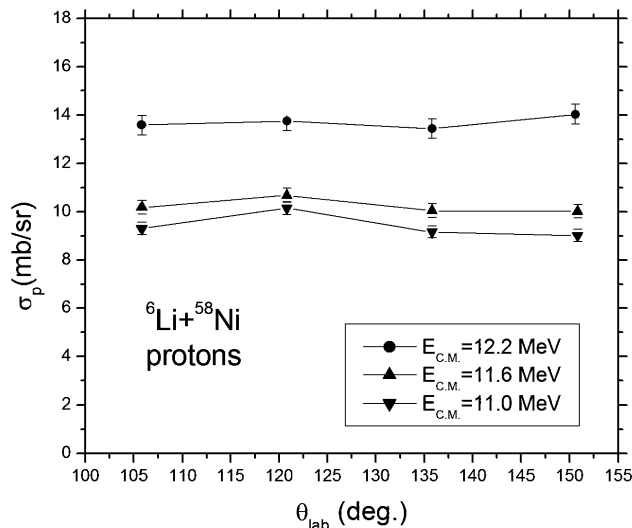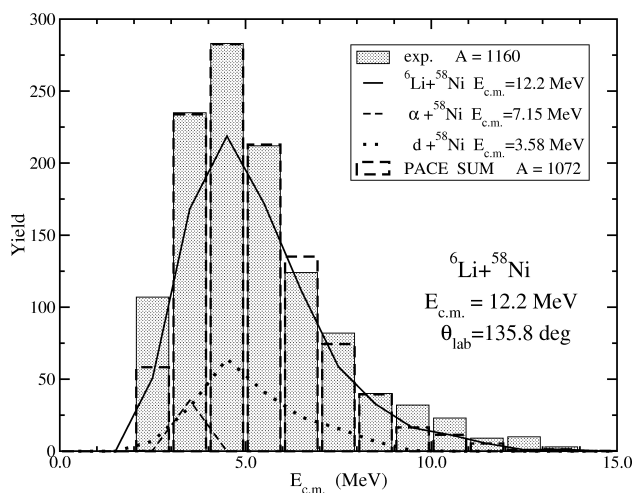FIGURE 3. Proton angular distributions from the ^{6}Li+^{58}Ni reaction.

TABLE I. Fusion Barriers (V_0) and proton multiplicities for selected energies.

Reaction	V_0 (MeV)	$E_{c.m.}$ (MeV)	m_p
^{6}Li + ^{58}Ni	12.5	11.0	1.42
		12.2	1.40
d + ^{58}Ni	4.4	3.2	0.81
		3.6	0.81
α + ^{58}Ni	8.6	6.4	0.96
		7.2	0.93
^{8}B + ^{58}Ni	20.8	22.0	2.47
		25.0	2.54
^{7}Be + ^{58}Ni	16.7	19.1	1.93
		21.7	2.05
p + ^{58}Ni	4.7	2.7	1.00
		3.1	1.00

FIGURE 4. Proton spectrum.
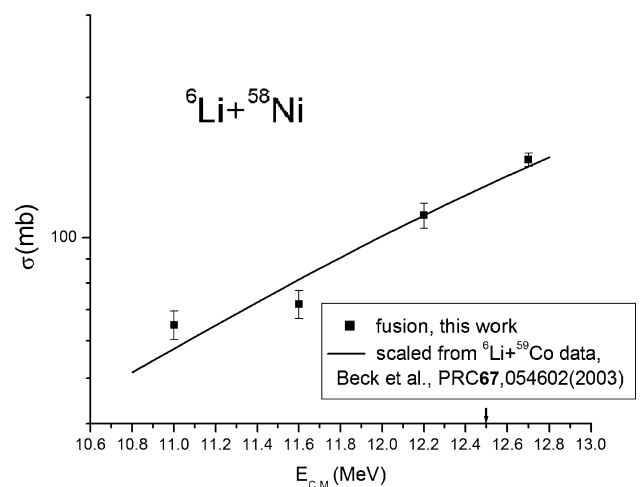

FIGURE 5. Fusion excitation function for ^{6}Li+^{58}Ni.

The good agreement of our data with this curve supports the validity of the present technique to obtain the fusion cross sections.

The technique was then applied to the analysis of the $^8B+^{58}Ni$ reaction, obtaining angular distributions such as shown in Fig. 6 and spectra such as the one in Fig. 7. As was the case for Li+Ni, here again the angular distributions for the four measured angles and the proton spectra are properly described by the statistical model (PACE) if both, CF and ICF processes are considered, in this case assuming that ^8B can be thought of as a ^7Be core plus one proton (the presumptive one-proton halo).

In addition, model dependency was tested in this case by varying in PACE the level density parameter a within extreme values ($A/10 \le a \le A/7$) [17] and by using alternatively the parameterization of Gilbert and Cameron [17, 18]. The maximum variation of about 10% obtained in the multiplicities is consistent with the intuitive idea that, for proton (or neutron) rich systems, the nucleus first tries to emit protons (or neutrons) so the predicted multiplicity is more stable than cases where the nucleus has more options for decay.
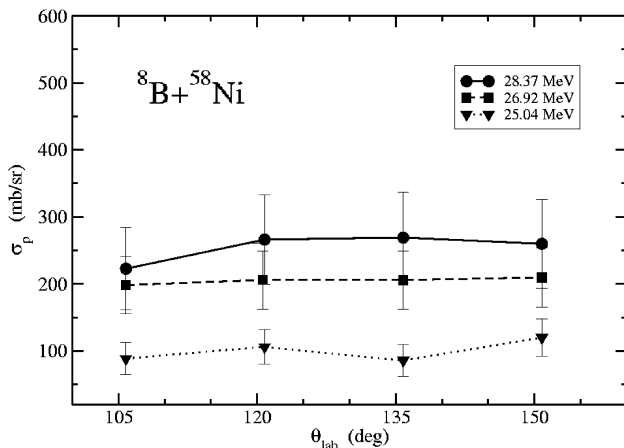
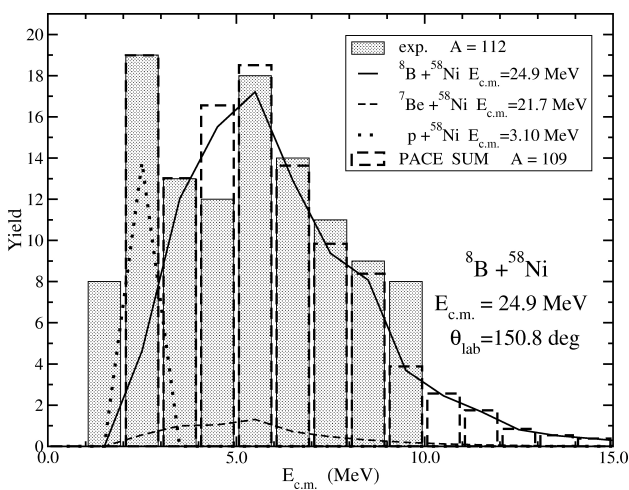

FIGURE 6. Proton angular distributions for $^8B+^{58}Ni$.

FIGURE 7. Proton energy-distribution for $^8B+^{58}Ni$.
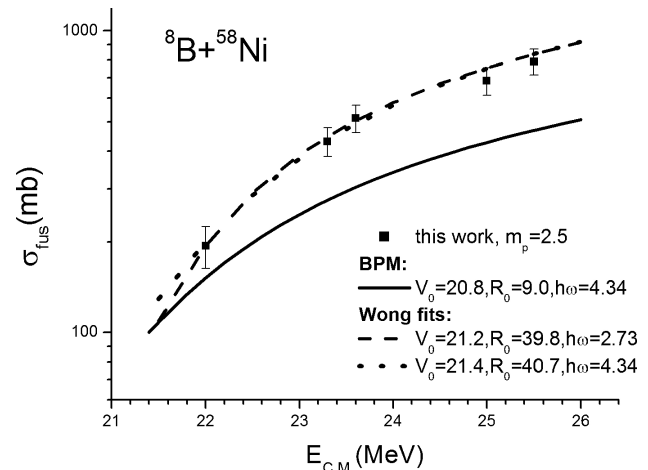

FIGURE 8. Fusion excitation function for $^8B+ {}^{58}Ni$. The curves are described in the text.

Using the multiplicities of Table I, the obtained fusion excitation function is presented in Fig. 8. The solid line in this figure is a one-dimensional barrier penetration model (BPM) calculation using the barrier height indicated in Table I, which by comparison with the data indicates a large fusion enhancement. The dashed line is a three parameter fit of the data with Wong's function [19]:

$$\sigma_W(E) = \frac{\hbar\omega R_0^2}{2E} ln \left[1 + exp \frac{2\pi}{\hbar\omega}(E - V_0) \right] \qquad (1)$$

which gives the barrier parameters V_0=21.2 MeV, R_0=39.8 fm, $\hbar\omega$= 2.73 MeV. The striking result is the large barrier radius needed to fit the data. Fixing one of the parameters gives similar results; in the dotted curve, for example, the curvature parameter was kept fixed at $\hbar$=4.34 MeV and the remaining two parameters were fit, giving again a very large radius (40.7 fm). This result is consistent with the finding in Ref. [5], mentioned in the introduction, that even at very large distances the Coulomb-nuclear interference is important, and could perhaps be taken as an additional evidence for the proton-halo nature of ^8B.

4. Conclusions

Proton angular-distributions were obtained for ^6Li, ^8B + ^{58}Ni at 4 energies. The spectra were generally consistent with fusion(CF+ICF)-evaporation calculations. The method showed a potentiality to separate CF from ICF contributions.

Using PACE-multiplicities to estimate σ_{fus}, the results for ^6Li agree with previous measurements for $^6Li+^{59}Co$ (properly scaled) and the results for ^8B are surprisingly high, implying a huge barrier radius, supporting previous evidence of a proton-halo nature for ^8B.

Acknowledgments

* e-mail: efar@nuclear.inin.mx.

1. J. N. Bahcall, *Neutrino Astrophysics* (Cambridge University Press, New York, 1989).

2. J. von Schwarzenberg, J. J. Kolata, D. Peterson, P. Santi, M. Belbot, and J. D. Hinnefeld, *Phys. Rev. C* **53** (1996) R2598.

3. H. Kitagawa and H. Sagawa, *Phys. Lett. B* **299** (1993) 1.

4. H. Nakada and T. Otsuka, *Phys. Rev. C* **49** (1994) 886.

5. V. Guimaraes, et al., *Phys.Rev. Lett.* **8** (2000) 1862.

6. J. J. Kolata, et al., *Phys. Rev. C* **63** (2001) 024616.

7. J. J. Kolata, V. Guimaraes, D. Peterson, P. Santi, R. White Stevens, P. A. DeYoung, G. F. Peaslee, B. Hughey, B. Atalla, M. Kern, P. L. Jolivette, J. A. Zimmerman, M. Y. Lee, F. D. Becchetti, E. F. Aguilera, E. Martinez-Quiroz, and J. D. Hinnefeld, *Phys. Rev. Lett.* **81** (1998) 4580.

8. E. F. Aguilera, J. J. Kolata, F. M. Nunez, F. D. Becchetti, P. A. DeYoung, M. Goupel, V. Guimaraes, B. Hughey, M. Y. Lee, D. Lizcano, E. Martinez-Quiroz, A. Nowlin, T. OïDonnell, G. F. Peaslee, D. Peterson, P. Santi, and R. White Stevens, *Phys. Rev. Lett.* **84** (2000) 5058.

9. P. A. DeYoung, B. Atallah, B. Hughey, P. L. Jolivette, M. Kern, G. F. Peaslee, J. J. Kolata, V. Guimaraes, D. Peterson, P. Santi, R. White-Stevens, E. F. Aguilera, E. Martínez-Quiroz, F. D. Becchetti, M. Y. Lee, J. A. Zimmerman, J. D. Hinnefeld, and O. A. Capurro, *Phys. Rev. C* **62** (2000) 047601.

10. E. F. Aguilera, J. J. Kolata, F. D. Becchetti, P. A. DeYoung, J. D. Hinnefeld, A. Horvath, L. O. Lamm, Hye-Young Lee, D. Lizcano, E. Martínez-Quiroz, T. W. O'Donnell, D. A. Roberts, and G. Rogachev, *Phys. Rev. C* **63** (2001) 061603(R).

11. J.P. Bychowski, P.A. DeYoung, B.B. Hilldore, J.D. Hinnefeld, A. Vida, F.D. Becchetti, J. Lupton, T.W. O'Donnell, J.J. Kolata, G. Rogachev, and M. Hencheck, *Phys. Lett. B,* **596** (2004) 26.

12. K.E. Rehm et al., *Phys. Rev. Lett.* **81** (1998) 3341.

13. J.F. Liang, et al., *Phys. Lett B* **491** (2000) 23.

14. M. Y. Lee et al., *Nucl. Instrum. Methods Phys. Res.,* Section A **422** (1999) 536.

15. A. Gavron, *Phys. Rev. C* **21** (1980) 230.

16. Beck et al., *Phys. Rev. C* **67** (2003) 054602.

17. R. G. Stokstad, *Treatise on Heavy-Ion Science*, vol. 3, Ed. D. A. Bromley (1985) p.83.

18. A. Gilbert and A. G. W. Cameron, *Can. J. Phys.* **43** (1965) 1446.

19. C. Y. Wong, *Phys. Rev. Lett.* **31** (1973) 766.